INTERFACE

royalsocietypublishing.org/journal/rsif

Research

Cite this article: Latash EM, Barnett WH, Park H, Rider JM, Klishko AN, Prilutsky BI, Molkov YI. 2020 Frontal plane dynamics of the centre of mass during quadrupedal locomotion on a split-belt treadmill. *J. R. Soc. Interface* **17**: 20200547.
http://dx.doi.org/10.1098/rsif.2020.0547

Received: 10 July 2020
Accepted: 14 August 2020

Subject Category:
Life Sciences–Mathematics interface

Subject Areas:
computational biology, biomechanics, biomathematics

Keywords:
locomotion, centre of mass, inverted pendulum, dynamic stability, split-belt treadmill

Authors for correspondence:
B. I. Prilutsky
e-mail: boris.prilutsky@biosci.gatech.edu
Y. I. Molkov
e-mail: ymolkov@gsu.edu

†These authors share senior authorship.

Electronic supplementary material is available online at https://doi.org/10.6084/m9.figshare.c.5099245.

THE ROYAL SOCIETY PUBLISHING

Frontal plane dynamics of the centre of mass during quadrupedal locomotion on a split-belt treadmill

E. M. Latash[1], W. H. Barnett[1], H. Park[3], J. M. Rider[1], A. N. Klishko[4], B. I. Prilutsky[4,†] and Y. I. Molkov[1,2,†]

[1]Department of Mathematics and Statistics, and [2]Neuroscience Institute, Georgia State University, Atlanta, GA, USA
[3]Department of Electrical and Computer Engineering, Texas A&M University, College Station, TX, USA
[4]School of Biological Sciences, Georgia Institute of Technology, 555 14th street NW, Atlanta 30332, GA, USA

EML, 0000-0001-8532-2233; BIP, 0000-0003-0499-3890; YIM, 0000-0002-0862-1974

Our previous study of cat locomotion demonstrated that lateral displacements of the centre of mass (COM) were strikingly similar to those of human walking and resembled the behaviour of an inverted pendulum (Park *et al.* 2019 *J. Exp. Biol.* **222**, 14. (doi:10.1242/jeb.198648)). Here, we tested the hypothesis that frontal plane dynamics of quadrupedal locomotion are consistent with an inverted pendulum model. We developed a simple mathematical model of balance control in the frontal plane based on an inverted pendulum and compared model behaviour with that of four cats locomoting on a split-belt treadmill. The model accurately reproduced the lateral oscillations of cats' COM vertical projection. We inferred the effects of experimental perturbations on the limits of dynamic stability using data from different split-belt speed ratios with and without ipsilateral paw anaesthesia. We found that the effect of paw anaesthesia could be explained by the induced bias in the perceived position of the COM, and the magnitude of this bias depends on the belt speed difference. Altogether, our findings suggest that the balance control system is actively involved in cat locomotion to provide dynamic stability in the frontal plane, and that paw cutaneous receptors contribute to the representation of the COM position in the nervous system.

1. Introduction

Quadrupedal animals must coordinate the motion of limbs in order to maintain balance. Balance is controlled by keeping the position of the centre of mass (COM) between the weight-bearing limbs; e.g. [2]. Animals are said to be statically stable when the COM projection is within the edges of support [2,3]. While this may seem trivial for a quadruped standing at rest [4], it becomes more complicated when the animal begins to move. Animals are said to be dynamically stable when the extrapolated centre of mass (xCOM) projection is within the edges of support [3]. During walking, quadrupedal animals must continuously maintain balance in both the lateral and longitudinal directions. For example, walking cats are statically unstable laterally and dynamically unstable longitudinally during ipsilateral and diagonal double-support phases, respectively [5].

The lateral control of balance is particularly important in bipedal locomotion, e.g. in walking ducks [6], penguins [7], non-human primates [8] and humans [9,10], where the moving animal is only supported by a single limb for most of the walking cycle. During phases of single-limb support, the body may be modelled as an inverted pendulum [11]. According to this model, lateral balance is maintained by timely placing the swing limb on the ground to stop the body, falling under the action of the gravitational moment, and changing the pivot point of the inverted pendulum and thus the direction of the gravitational moment with each step [11,12]. To plan the timing and position of limb placement, the balance control system must have knowledge of the mechanical state of the walker, i.e. the COM position and velocity with respect to the boundaries of support [3,13]. This information is probably obtained from the integration of visual, vestibular, proprioceptive and cutaneous afferent signals [14], although the contribution of individual sensory modalities to the integrated sensory input is still uncertain.

Though derived in the context of bipedal locomotion, the inverted pendulum principles could potentially be extended and applied to quadrupedal walking. For example, the kinetic and potential energies of the body in the sagittal plane show out-of-phase changes in the walking cycle of dogs, macaques and rams, resembling the behaviour of an inverted pendulum [15,16]. Frontal plane COM motion resembles that of bipeds in long-legged quadrupeds: dogs [17], camels [18], giraffes [19] and alpacas [20], who use a pace-like walking gait, in which the phase difference between the ipsilateral hindlimb and forelimb footfalls approaches zero [21]. During pace walking, the animal body is supported mostly by either pair of ipsilateral limbs. Nevertheless, the majority of quadrupedal animals during medium-speed walking use a lateral sequence of limbs to support the body with either two or three feet on the ground at all times. For example, in cats walking overground at speeds approximately 0.4–1.0 m s^{-1}, the ipsilateral limb phase difference is 0.25–0.30 of the cycle duration [22,23]. During cat treadmill walking, on the other hand, this phase difference is much smaller ≤0.15 [22,24], so the COM frontal plane dynamics of cats walking on a treadmill could be similar to those of bipeds and inverted pendulum.

Indeed, we have demonstrated in cats walking on a treadmill [1] that lateral displacements of the COM and xCOM [3], with respect to the borders of support (centre of pressure, COP) are strikingly similar to those of humans [12,25] and thus could potentially be explained by the dynamics of an inverted pendulum. The results of our previous study have also suggested that cats regulate lateral balance by controlling the timing of the ipsilateral double-support phase onset (or the timing of swing onset of the contralateral forelimb). However, the extent to which frontal plane dynamics of the cat walking on a treadmill can be explained by the inverted pendulum model has not been rigorously investigated.

The goal of this study was to investigate if an inverted pendulum-based model can reproduce major features of the frontal plane COM dynamics of cats walking on a treadmill. The second goal was to use this model to interpret the effects of experimental perturbations of lateral stability. We used two types of perturbations: (i) different speed ratios of the left and right treadmill belts during split-belt locomotion; and (ii) unilateral paw pad anaesthesia. Increasing belt speed asymmetry during split-belt treadmill locomotion leads to the reduction of the lateral margins of dynamic stability on the slower side in both humans [26,27] and cats [1]. Cutaneous feedback from the feet has been implicated in the regulation of lateral balance in cats [28,29] and humans [30,31]. Therefore, we expected that compromising cutaneous feedback from paw pads by anaesthesia unilaterally would impact lateral balance dynamics. By modelling the cat COM lateral dynamics in the range of these experimental perturbations, we hoped to understand better the mechanisms of balance control in the frontal plane and, in particular, contributions of cutaneous feedback in this control.

2. Methods

2.1. Experimental data collection

All experimental procedures were consistent with the Principles of Laboratory Animal Care (publication of the National Research Council of the National Academies, 8th edition, 2011) and approved by the Georgia Tech Institutional Animal Care and Use Committee (protocol numbers A100012DO and A100011UV).

Animal subjects and all experimental procedures and conditions were the same as in our previous study [1], so only their brief description is provided here. Four adult female cats with mass ranging from 2.55 to 4.10 kg took part in the experiments. After 3- to 4-week training with a food reward, each cat walked on a split-belt treadmill (Bertec Corporation, Columbus, OH, USA) at four-speed combinations of the left and right treadmill belts. In the control condition, cats walked on a treadmill with equal split-belt speeds of 0.4 m s^{-1} (speed ratio 1 : 1). The speed of the right belt was increased by a factor of 1.5 to 0.6 m s^{-1} and by two times to 0.8 m s^{-1} for two additional split-belt speed ratios (0.4 m s^{-1}: 0.6 m s^{-1} or 1 : 1.5 and 0.4 m s^{-1}: 0.8 m s^{-1} or 1 : 2). In the last speed condition, the speed of the left belt was increased by two times to 0.8 m s^{-1}, while the right belt was kept at 0.4 m s^{-1} (0.8 m s^{-1}: 0.4 m s^{-1} or 2 : 1). In each split-belt condition, the cat first walked for 15 s at equal belt speeds of 0.4 m s^{-1}; subsequently, the speed ratio was changed to the desired value within 1 s, maintained for 60 s, then returned to the initial equal speed condition within 1 s and maintained for additional 15 s. The order of the tested split-belt speed conditions was randomized within each animal.

For additional perturbation of lateral balance by compromising cutaneous feedback from paw pads (see Introduction), the same split-belt speed conditions were tested with unilateral paw pad anaesthesia on a separate day. The order of testing sessions with and without anaesthesia was randomized across animals. Paw anaesthesia was administered using lidocaine injections in each pad of the right forepaw and right hindpaw. The anaesthesia caused the removal of cutaneous sensory feedback from the right paws for about 30 min, during which time the locomotion testing was performed; for details see [1].

During locomotor experiments, three-dimensional coordinates of 28 markers, placed bilaterally on the metatarsophalangeal, ankle, knee and hip joints of the hindlimbs; metacarpophalangeal, wrist, elbow and shoulder joints of the forelimbs; and the head, were recorded with a six-camera motion-capture system (Vicon, UK) at a sampling rate of 250 Hz. Recorded marker coordinates (filtered by a fourth-order Butterworth zero-lag filter, cut-off frequency 15 Hz) and three-dimensional mechanical model of the cat body were used to compute the COM coordinates; for details see [23,32].

2.2. Experimental data analysis

We used computed COM and paw positions as functions of time to derive relevant parameters of the model. Specifically, we defined the period of lateral COM oscillations (P) as the duration of the cycle, the amplitude of lateral COM oscillations (A_{COM}) as half of the difference between the maximum and minimum lateral coordinate of the COM during one cycle, the lateral positions of left and right hindpaws (LH and RH) and the lateral COM position relative to the left hindpaw position normalized to the hindpaw step width (Z_{COM}); figure 1*a*. We selected for analysis contiguous 60 s motion recordings of each split-belt condition, removing the first 10 s of each recording, during which walking was less regular. This irregularity normally occurred within the first 5 s after the 1 s speed change from the initial speed ratio of 1 : 1. We observed no motor adaptation to asymmetric belt speeds in terms of step length, step duration and duty cycle. That was consistent with a previous report of the lack of motor adaptation to prolonged split-belt locomotion in cats [33]. Recordings were divided into stride cycles, defined by the moment of right hindpaw placement on the ground. Each parameter was determined in each cycle of each experimental condition and each animal.

Average COM position was calculated for each cycle by taking the average value of the COM coordinates across all timepoints within a single cycle. The average COM position for a

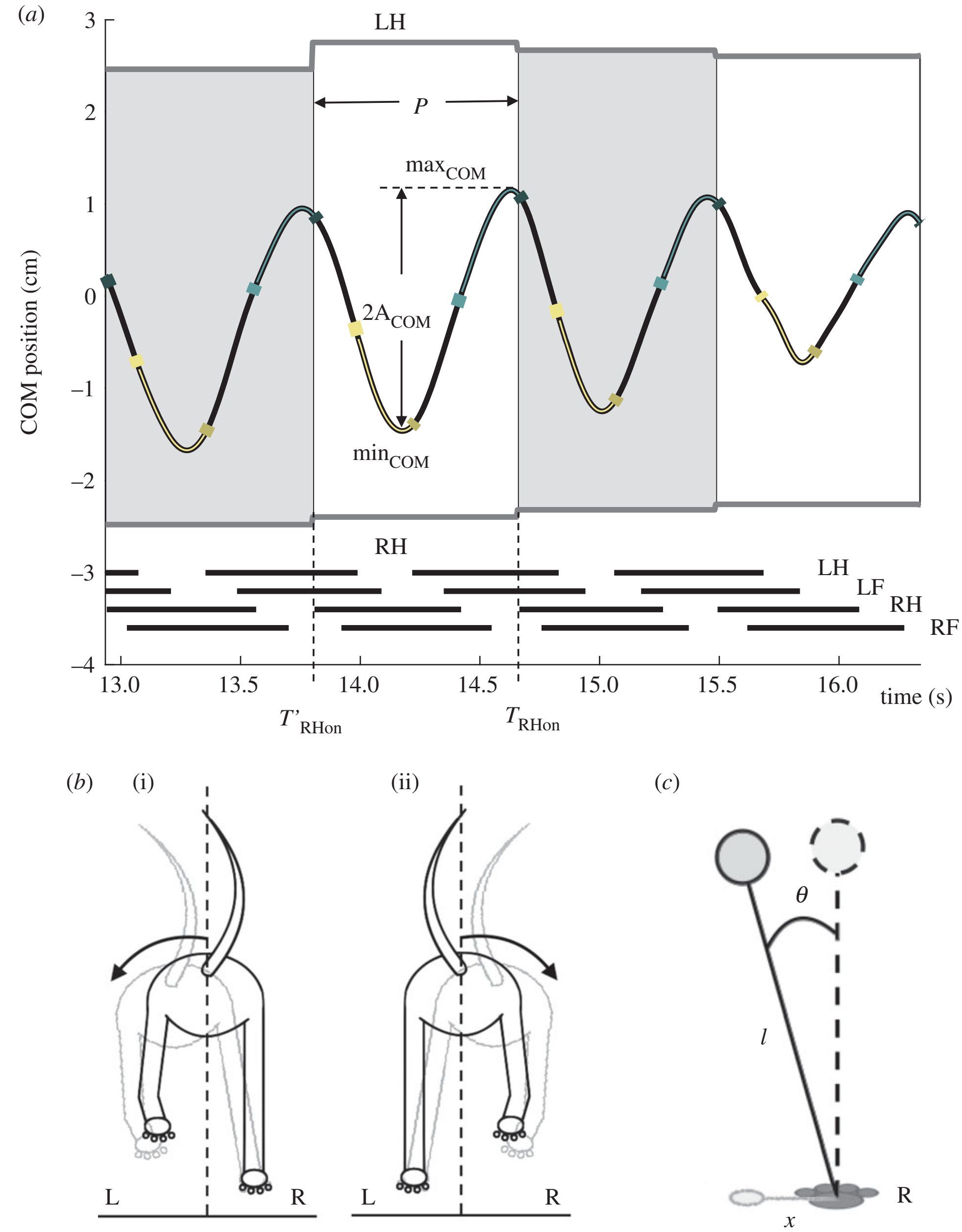

Figure 1. Data processing and modelling notations. (*a*) Definition of COM kinematic parameters. The oscillating line corresponds to the lateral displacement of the COM during selected strides of treadmill locomotion with symmetric belt speeds (40 cm s^{-1}; cat no. 03, without anaesthesia). Positive and negative COM values correspond to displacements in the left and right directions. Square marks in the COM oscillations show the time of hindpaw lift and placement on the ground for the right hindpaw in turquoise and the left hindpaw in khaki. Positions of the top and bottom sides of each rectangle correspond to the mean lateral position of the left and right hindpaw averaged over the cycle. The height of grey and white rectangles corresponds to the mean hindpaw step width in each cycle. Horizontal thick lines at the bottom indicate the stance period of each limb; left hind (LH), left fore (LF), right hind (RH) and right fore (RF) limbs. The thickness of the rectangles is the step cycle period, *P*, defined by timing of right hindlimb placements on the ground (T'_{RHon} and T_{RHon}). The amplitude, A_{COM}, is half of the distance between the maximum and minimum COM points in one cycle. (*b*) Body oscillations. The direction of the body movement is depicted by arrows. When the left (L) paws are lifted, the body is dragged to the left by the gravitational moment. When the right (R) paws are lifted, the body is dragged to the right. (*c*) The inverted pendulum approximation. The inverted pendulum swings at an angle θ from the vertical in the frontal plane. The length of the pendulum is *l* and the lateral displacement of the COM vertical projection is *x*.

subject in one condition was obtained by averaging across all cycles in a single recording. Standard error values were calculated across subjects in a single condition. The equations for the above locomotor parameters are listed below:

$$P = T_{RHon} - T'_{RHon}, \tag{2.1}$$

$$A_{COM} = \frac{max_{COM} - min_{COM}}{2}, \tag{2.2}$$

and

$$Z_{COM} = \frac{LH - COM}{LH - RH}, \tag{2.3}$$

where P is the stride cycle period; T_{RHon} and T'_{RHon} are the times of the current and previous stance onsets of the right hindpaw, respectively; A_{COM} is the COM oscillation magnitude in the lateral direction; max_{COM} and min_{COM} are the maximum and minimum values of the COM lateral displacement in the cycle; Z_{COM} is the average normalized lateral COM position; LH and RH are the lateral positions of the left and right hindpaws, respectively (figure 1*a*).

2.2. Model development

For the stationary cat to remain upright, the COM vertical projection must stay between the borders of support on either side. However, if the COM is moving with some lateral velocity v, this could make the cat dynamically unstable. Which is to say that v must not exceed the value at which, xCOM, crosses the border of support, or the animal will not be able to suppress its lateral motion to prevent the COM from moving beyond the border of support. The xCOM is defined as $\mathrm{xCOM} = \mathrm{COM} + v/\omega$, where $\omega = \sqrt{g/l}$, g is the acceleration due to gravity, and l is the maximum height of the COM [3]; see figure 1*b*,*c*.

Presume that the cat makes balance control decisions based upon the xCOM position in order to maintain dynamic stability. The limb lift-off times on either side would be determined by some position thresholds p_L and p_R of xCOM such that p_R defines the transition from the support on both sides (two-side support) to unilateral stance on the right side; p_L defines the transition from the two-side support to unilateral stance on the left side. In this case, the decision-making thresholds would still be determined during the two-side support phases. During these phases, the state of dynamic stability would be defined by the inequalities $p_R < \mathrm{xCOM} < \mathrm{p_L}$. Given the definition of xCOM, we can rewrite these expressions to be $p_R < \mathrm{COM} - q/\omega$ and $\mathrm{COM} + q/\omega < p_L$ $(q = |v|)$ taking into account the direction of COM movement. Based on our previous study, we made an assumption that the lateral speed of the COM is roughly constant during and across intervals of support on both sides of the body, which occur during either three-limb support or diagonal two-limb support phases; see figs 1a and 8a in [1]. Because q is constant, the decision-making thresholds can be formulated for COM rather than xCOM position as follows:

$$s_R < \mathrm{COM} < s_L\ , \tag{2.4}$$

where $s_R = p_R + q/\omega, s_L = p_L - q/\omega$.

Over the course of a complete stride cycle, the equations of motion that govern the lateral position of COM are determined by the decision-making thresholds s_L and s_R. These thresholds represent the lateral coordinates of the COM at which the cat ipsilateral limbs transition to and from the phases of the two-side support (phases 1 and 3 in figure 2) and unilateral swing or contralateral stance (phases 2 and 4; figure 2).

During phase 1, the cat is supported by the limbs on both sides of the body, and the dynamics of the lateral COM coordinate x is determined by $\mathrm{d}x/\mathrm{d}t = -q$ with an initial condition $x(0) = s_L$. phase 1 lasts until the COM crosses the threshold s_R. Because the COM travels with constant velocity $-q$, the duration of this interval can be written as $T_1 = (s_L - s_R)/q$, and its equation of motion is

$$x(t) = s_L - qt. \tag{2.5}$$

Then, the cat swings the left limbs as the COM crosses the threshold s_R, transitioning the model into phase 2.

During phase 2, the left limbs are in the swing, and the COM accelerates in the leftward direction away from the position of unilateral support on the right side. In this phase, the dynamics of COM is determined by the inverted pendulum equation:

$$\frac{\mathrm{d}^2x}{\mathrm{d}t^2} = \omega^2(x + h), \tag{2.6}$$

where $-h$ is the coordinate of the right paw. When phase 2 begins, the model inherits its initial conditions from the previous phase:

$$x(T_1) = s_R,\quad x'(T_1) = -q. \tag{2.7}$$

The equation of motion of the COM during phase 2 is

$$x(t) = -h + (h + s_R)\cosh(\omega(t - T_1)) - \frac{q}{\omega}\sinh(\omega(t - T_1)). \tag{2.8}$$

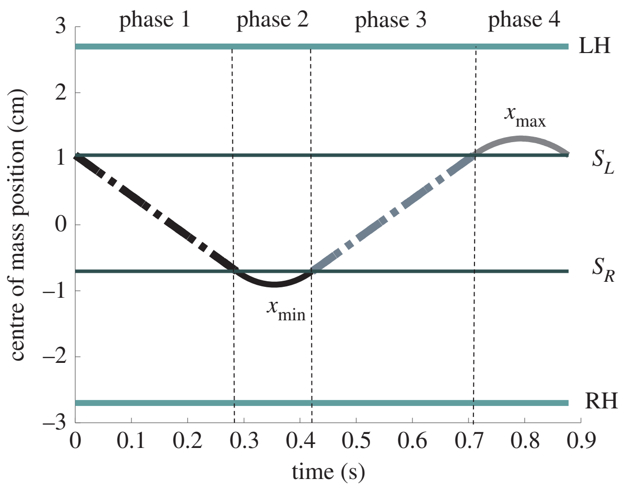

Figure 2. phases of lateral COM displacement in a walking cycle. The COM position is shown as a function of time in a walking cycle. Upward and downward directions correspond to displacements to left and right, respectively. Green thick lines at 2.7 cm and −2.7 cm show the average position of left and right hindpaws, labelled as LH and RH, respectively. During phase 1, the COM moves from left to right from threshold s_L to threshold s_R with constant speed. At threshold s_R, the left paws are lifted. During phase 2, the COM first continues moving right at threshold s_R, but changes direction in mid phase and starts moving leftwards to threshold s_R owing to the action of the gravitational moment and then it crosses s_R when the left paws are placed back on the ground. In phase 3, the COM moves from right to left from threshold s_R to threshold s_L at constant speed. At threshold s_L, the right paws are lifted. During phase 4, the COM first continues moving left at threshold s_L, but then changes direction in mid phase and starts moving rightwards to threshold s_L owing to the action of the gravitational moment.

The minimum of the COM coordinate is

$$x_{\min} = -h + \sqrt{(h + s_R)^2 - \frac{q^2}{\omega^2}}, \tag{2.9}$$

and the duration of phase 2 is

$$T_2 = \frac{1}{\omega}\ln\frac{\omega(h + s_R) + q}{\omega(h + s_R) - q}. \tag{2.10}$$

phase 2 ends as the COM crosses threshold s_R, entering a phase of dual support (phase 3).

In phase 3, the cat once more has support on both the left and right sides of the body, and the dynamics is determined by the equation $\mathrm{d}x/\mathrm{d}t = q$, and its initial condition is $x(T_1 + T_2) = S_R$. The time it takes the COM to traverse the distance between the two decision-making thresholds is $T_3 = (s_L - s_R)/q$, and its equation of motion is

$$x(t) = s_R + q(t - T_1 - T_2). \tag{2.11}$$

At the end of phase 3, the right limbs are lifted as the COM crosses the threshold s_L, and the model enters phase 4.

While the right limbs are in swing phase, the COM accelerates away from the position of support provided by the left limbs:

$$\frac{\mathrm{d}^2x}{\mathrm{d}t^2} = \omega^2(x - h), \tag{2.12}$$

where h is the coordinate of the left paw. At the beginning of phase 4, the initial conditions are

$$x(T_1 + T_2 + T_3) = s_L \quad \text{and} \quad x'(T_1 + T_2 + T_3) = q.$$

The equation of motion during phase 4 is

$$x(t) = h - (h - s_L)\cosh(\omega(t - T_1 - T_2 - T_3)) + \frac{q}{\omega}\sinh(\omega(t - T_1 - T_2 - T_3)). \quad (2.13)$$

The maximum COM displacement during phase 4 is

$$x_{\max} = h - \sqrt{(h - s_L)^2 - \frac{q^2}{\omega^2}}, \quad (2.14)$$

and the duration of phase 4 is

$$T_4 = \frac{1}{\omega}\ln\frac{\omega(h - s_L) + q}{\omega(h - s_L) - q}. \quad (2.15)$$

In this way, the thresholds s_L and s_R determine the position of COM at which two-side support changes to unilateral support.

Given these expressions, we can analytically compute the quantities $A_{\mathrm{COM}}(s_L, s_R, q)$, $P(s_L, s_R, q)$ and $Z_{\mathrm{COM}}(s_L, s_R, q)$ for our model as functions of model parameters s_L, s_R and q. The amplitude of the oscillatory solution is

$$A_{\mathrm{COM}}(s_L, s_R, q) = \frac{x_{\max} - x_{\min}}{2}, \quad (2.16)$$

and the period of the oscillatory solution is

$$P(s_L, s_R, q) = T_1 + T_2 + T_3 + T_4. \quad (2.17)$$

The average COM position is defined over cycle as

$$\overline{\mathrm{COM}} = \frac{1}{P}\int_0^P x(t)\,\mathrm{d}t, \quad (2.18)$$

which we normalize to the relative position in the base of support:

$$Z_{\mathrm{COM}}(s_L, s_R, q) = \frac{h - \overline{\mathrm{COM}}}{2h}, \quad (2.19)$$

where h is the distance from the midline to the support position on either side.

2.3. Model parameter inference

After processing the experimental data as described above, we obtained average values of the period, amplitude and normalized COM position, P, A, Z_{COM}, and their standard errors δP, δA, δZ for each experimental condition. To find the corresponding values of model parameters, we numerically solved the system of equations for s_L, s_R and q such that the model output in terms of period, amplitude and average COM position exactly matched the experimental measurements: $A_{\mathrm{COM}}(s_L, s_R, q) = A$, $P(s_L, s_R, q) = P$, and $Z_{\mathrm{COM}}(s_L, s_R, q) = Z_{\mathrm{COM}}$. We then computed standard errors for s_L, s_R, and q using Bayesian inference with uniform priors. The posterior probability density function for model parameters ($p.d.f.$) was therefore proportional to the likelihood function which was assumed Gaussian:

$$p.d.f. \sim \exp\left\{-\frac{1}{2}\left(\frac{(A - A(s_L, s_R, q))^2}{\delta A^2} + \frac{(P - P(s_L, s_R, q))^2}{\delta P^2} + \frac{(Z_{\mathrm{COM}} - Z_{\mathrm{COM}}(s_L, s_R, q))^2}{\delta Z^2}\right)\right\}. \quad (2.20)$$

The computed values for s_R and s_L were used to define parameters for model interpretation for each experimental condition. The distance between thresholds (DT) was defined as the difference between s_L and s_R. The threshold mean (TM) was the average of s_L and s_R. The change in threshold mean with anaesthesia ($\Delta\mathrm{TM_a}$) was the difference between TM with and without ipsilateral paw anaesthesia in one belt speed ratio.

2.4. Statistics

We used a mixed linear model analysis (IBM SPSS 24, Chicago, IL, USA) to determine the significance of the effects of cutaneous feedback and belt speed ratio on Z_{COM}, P, and A_{COM}. In the analysis, cutaneous feedback and belt speed ratio were within-subject independent factors. Animals and cycles were random factors. The main effect of independent factors and their interactions were determined at a significance level of 0.05. Pairwise comparisons of significant effects were performed with post hoc tests using the Bonferroni adjustment.

The significance of cutaneous feedback and belt speed ratio on model parameters was determined with z-tests. Z-scores were determined for model parameter estimates, s_R, s_L and q, as well as for other quantities used for model interpretation that depended on these parameters, DT, TM, $\Delta\mathrm{TM_a}$. Pairwise comparisons were performed at the 0.05 significance level.

We visualized the comparison of model trajectories to experimental waveforms by superimposing the COM positions across walking cycles for all subjects in one condition. Each walking cycle of a recording was divided into 100 bins. For each bin the mean and standard error of the COM position were calculated to characterize the average waveform and its distribution for each experimental condition. Then, a chi-square test was used to evaluate goodness-of-fit of the model.

3. Results

3.1. Model validation

Lateral COM displacements as simulated by the inverted pendulum were quantitatively similar to the mean COM displacements in different experimental conditions: belt speed ratios 1 : 1, 1 : 1.5 and 1 : 2 with and without unilateral paw anaesthesia (root mean square error (RMSE) < 0.01 cm; figure 3). See the electronic supplementary material, tables S1 and S2 for RMSE values and chi-squared test results for each condition.

3.2. Changes in centre of mass position with belt speed ratio and unilateral anaesthesia

The COM exhibited a left-right oscillatory motion during treadmill locomotion (figures 1 and 3). Experimental COM oscillatory motion parameters, A_{COM}, P and Z_{COM}, characterized the frontal plane COM dynamics. Z_{COM}, the lateral COM position averaged over the cycle shifted to the left (decreased, see equation (2.3)) as the belt speed ratio increased from 1 : 1 to 1 : 5 ($p < 0.05$) and from 1 : 1.5 to 1 : 2 ($p < 0.05$; figure 4*a*). At speed ratio 2 : 1 (at which the left and right belts moved at 0.8 m s^{-1} and 0.4 m s^{-1}, respectively), Z_{COM} showed a significant right shift compared to speed ratio 1 : 1. In trials with anaesthesia applied to the right paws, Z_{COM} shifted significantly to the right (the values increased; $p < 0.05$) for the belt speed ratios 1 : 1.5, 1 : 2 and 2 : 1, but not for 1 : 1 (figure 4*a*). See the electronic supplementary material, tables S3 and S4 for all pairwise comparisons of Z_{COM}.

The amplitude of COM oscillations A_{COM} was also found to vary with the speed-belt ratio (figure 4*b*). A_{COM} decreased significantly as the belt speed ratio increased from 1 : 1 to 1 : 1.5, to 1 : 2, and to 2 : 1, as well as from 1 : 1.5 to 1 : 2 and to 2 : 1 ($p < 0.05$). No significant change in amplitude of oscillations was found between speed ratios 1 : 2 and the 2 : 1 ($p = 1.00$). A_{COM} did not change significantly in response to unilateral anaesthesia ($p = 0.990$).

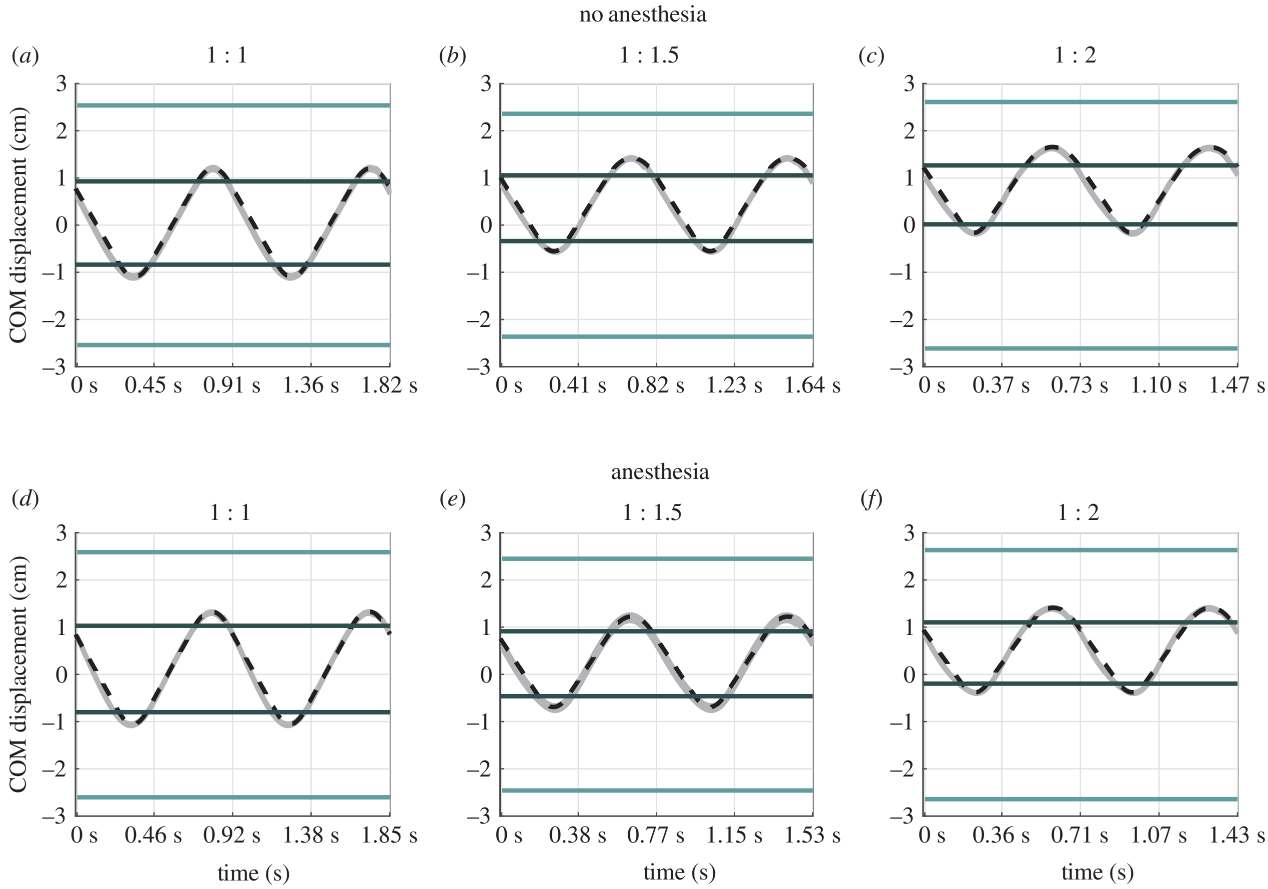

Figure 3. Comparison of lateral displacements of the model with the mean cat COM displacements in different experimental conditions. The model (black dashed lines) and experimental (continuous grey lines) displacements are shown for three belt speed ratios 1 : 1, 1 : 1.5 and 1 : 2 for intact paws (*a*,*b*,*c*) and unilateral paw anaesthesia (*d*,*e*,*f*). The experimental traces are the means computed across all cycles and cats; the thickness of the grey lines represents ± s.e. The dark grey horizontal lines are estimated lateral stability thresholds s_R (top) and s_L (bottom). The mean position of left and right limbs is shown in light blue. The total duration of each plot corresponds to two full cycle periods. All traces start at the onset of the unilateral right-limb support.

Stride cycle period, *P*, depended on the belt speed ratio (figure 4*c*). The step cycle period decreased from belt speed ratio 1 : 1 to 1 : 1.5, to 1 : 2, and to 2 : 1, as well as from ratio 1 : 1.5 to 1 : 2 and to 2 : 1 ($p < 0.05$). No significant difference in *P* was found between speed ratios 1 : 2 and 2 : 1 ($p = 0.082$). Unilateral anaesthesia did not induce a significant change in *P* ($p = 0.077$). See the electronic supplementary material, tables S5 and S6 for all pairwise comparisons of *P*, and tables S7 and S8 for all pairwise comparisons of A_{COM}.

3.3. Changes in stability thresholds with belt speed ratio and unilateral anaesthesia

The changes in model parameters were qualitatively similar to the mean experimental COM motion parameters in different experimental conditions: belt speed ratios 1 : 1, 1 : 1.5, 1 : 2 and 2 : 1 with and without unilateral paw anaesthesia (figure 3).

We observed a significant left shift of the estimated threshold for initiation of the left ipsilateral support, s_L, with changing the belt speed ratio from 1 : 1 to 1 : 2, from 1 : 1.5 to 1 : 2, and from 2 : 1 to 1 : 1, to 1 : 1.5 and to 1 : 2 for the unanaesthetized conditions ($p < 0.05$; figure 5*a*). The threshold for initiation of the right ipsilateral support, s_R, also shifted to the left with a change in speed ratio from 1 : 1 to 1 : 1.5 and to 1 : 2, from 1 : 1.5 to 1 : 2, and from 2 : 1 to 1 : 1.5 and to 1 : 2 ($p < 0.05$; figure 5*a*). There was also a much greater change of threshold s_R than s_L between speed ratios 1 : 1 through to 1 : 2, i.e. from −0.835 cm to 0.017 cm for s_R and from 0.931 cm to 1.266 cm for s_L. Anaesthesia of the right paws caused a significant right shift of threshold s_L at speed ratios 1 : 1.5 and 1 : 2, and of threshold s_R at speed ratios 1 : 2 and 2 : 1 ($p < 0.05$; figure 5*a*).

We did not detect significant changes in the model velocity parameter *q* with changes in speed ratio or paw anaesthesia conditions ($p > 0.05$; figure 5*b*).

Beacuse s_L and s_R depended differently on changes in the belt speed ratio, we quantified the net change in the COM dynamics by the threshold mean—the average of s_L and s_R at a given belt speed ratio and by the distance between thresholds—the difference of s_L and s_R at a given belt speed ratio (figure 6). The threshold mean significantly increased—indicating a shift to the left side—with a change in belt speed ratio when comparing 1 : 1 to 1 : 1.5 and to 1 : 2 belt speed ratios, as well as in the 1 : 1.5 to 1 : 2 and 2 : 1 belt speed ratio comparison ($p < 0.05$; figure 6*a*). The threshold mean significantly decreased with a change in belt speed ratio when comparing the 1 : 2 to the reverse 2 : 1 belt speed ratio ($p < 0.05$). The application of an anaesthesia to right-side paws significantly decreased the threshold mean at the 1 : 2 belt speed ratio, indicating a shift in the threshold mean towards the right side of the cat. However, when we considered the change in threshold mean in response to anaesthesia application across different speed ratios, we did not find significant differences among 2 : 1, 1 : 1.5 and 1 : 2 ratios ($p > 0.05$; figure 6*b*). The distance

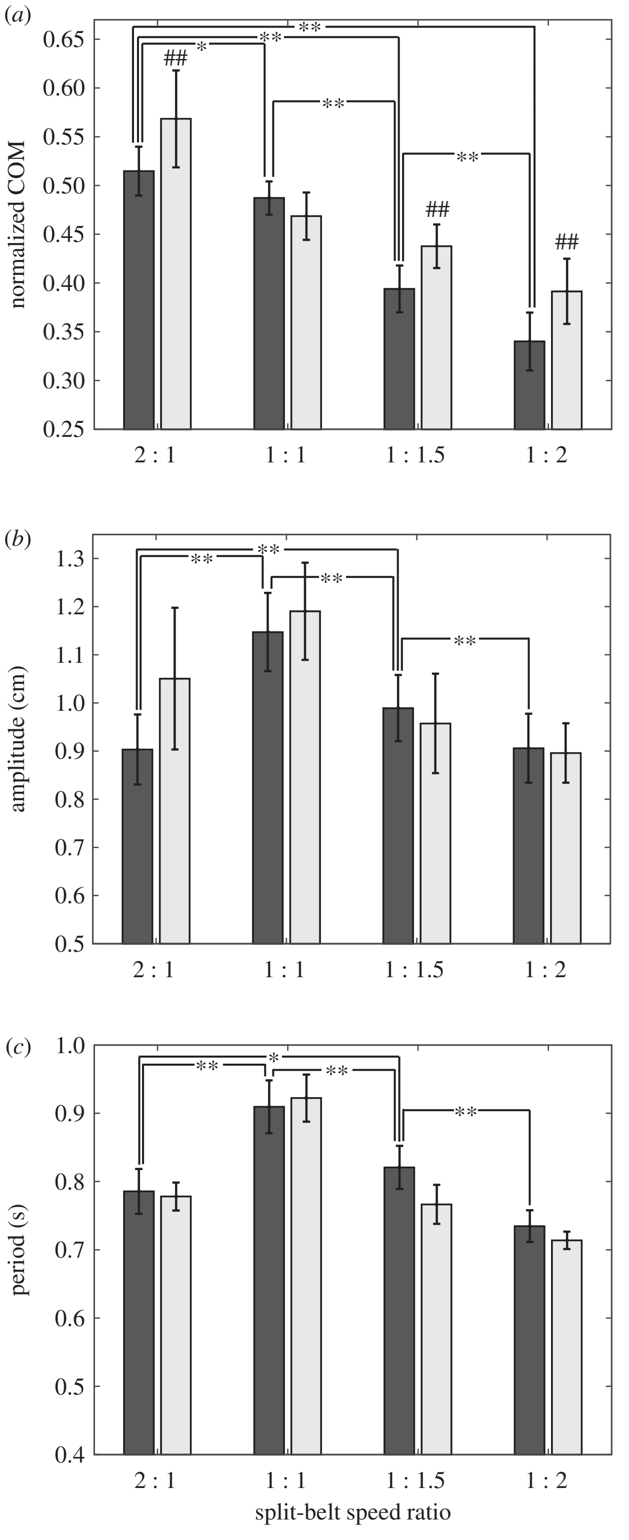

Figure 4. Mean normalized lateral COM position Z_{COM} in the cycle, COM oscillation amplitude A_{COM} and stride cycle period P as function of belt speed ratio and anaesthesia. Mean (±s.e.) were computed over all cats for each experimental condition. In each panel, an experimental measure is shown for split-belt speed ratios 2 : 1, 1 : 1, 1 : 1.5 and 1 : 2. Dark grey bars show results for intact paws; light grey bars show results for anaesthetized right paws. Asterisks depict significant effects of the speed ratios ($^*p < 0.05$, $^{**}p < 0.01$); hashtags (#) depict significant effects of the unilateral anaesthesia ($^{\#\#}p < 0.01$). (*a*) The COM position normalized to hindpaw step width, Z_{COM}. (*b*) COM oscillation amplitude, A_{COM}. (*c*) The cycle period, P.

between thresholds did not significantly change with belt speed, except for in the 1 : 1 to 1 : 2 belt speed ratio comparison. The distance between thresholds did not change significantly with the application of anaesthesia to the right paws ($p > 0.05$; figure 6*c*). See the electronic supplementary material, tables S9 through to 19 for pairwise comparisons of model parameters.

3.2. Effect of anaesthesia is independent of the sign of speed difference

We found that the change in threshold mean owing to anaesthesia in terms of its magnitude and direction was not statistically different across speed ratios of 2 : 1, 1 : 1.5 and 2 : 1 (figure 6*b*). To explore this further, we compared the changes in both thresholds s_L and s_R owing to right-side paw anaesthesia for speed ratios 2 : 1 and 1 : 2.

The change in the two thresholds owing to anaesthesia (Δs_L and Δs_R) was found to increase in magnitude with changes in belt speed ratio from 1 : 1 to 1 : 2 and 2 : 1 ($p < 0.05$). Additionally, the unilateral application of anaesthesia to the right side shifted the COM towards the anaesthetized side regardless of the speed-belt ratio of 1 : 2 or 2 : 1 (figure 7). There was no significant difference between changes in the thresholds for the two speed ratios ($p > 0.05$).

4. Discussion

The inverted pendulum-based model closely reproduced the experimentally measured COM lateral oscillations of cats walking on a split-belt treadmill with different belt speed ratios and with intact and unilaterally anaesthetized paws (figure 3). These results support the hypothesis that COM frontal plane dynamics of cats walking on a treadmill can be described by an inverted pendulum model.

We also tested the effect of varying belt speed ratios on COM lateral position and on lateral stability margins. As demonstrated in this (figures 3, 4*a* and 5*a*) and other recent studies in cats [1] and humans [26,27], the COM and xCOM shift towards the slower moving split-belt. We found that with a progressive change in belt speed ratio, the increase of the lateral stability margins on the faster moving side is much greater than the decrease of the stability margins on the slower side (figure 5*a*). Thus, the belt speed difference affected the lateral stability margins on the faster and slower sides asymmetrically. The same asymmetric changes in margins of stability have been reported for human split-belt walking [26] (see their fig. 2*a*). The authors have demonstrated (see also [12]) that these results are expected from the dynamics of an inverted pendulum model. In particular, the model predicts an inverse relationship between the duration of the unilateral support phase and the margin of stability on that side. Assuming that the unilateral support phase on the faster moving side of the treadmill is shorter, and therefore the stability margin is greater, the cycle-averaged xCOM should shift away from the faster moving leg. On the other hand, humans and presumably cats can voluntarily increase or decrease margins of stability by, for example, walking with a wide or narrow step width to minimize the risk of falling in an unstable environment or to satisfy task demands [5,23,34,35]. However, both humans and cats prefer shifting COM towards a slower belt. It is likely, therefore, that other factors besides the inverse pendulum dynamics can affect the asymmetric margins of stability during split-belt walking. One of such factors could be energy expenditure, see for

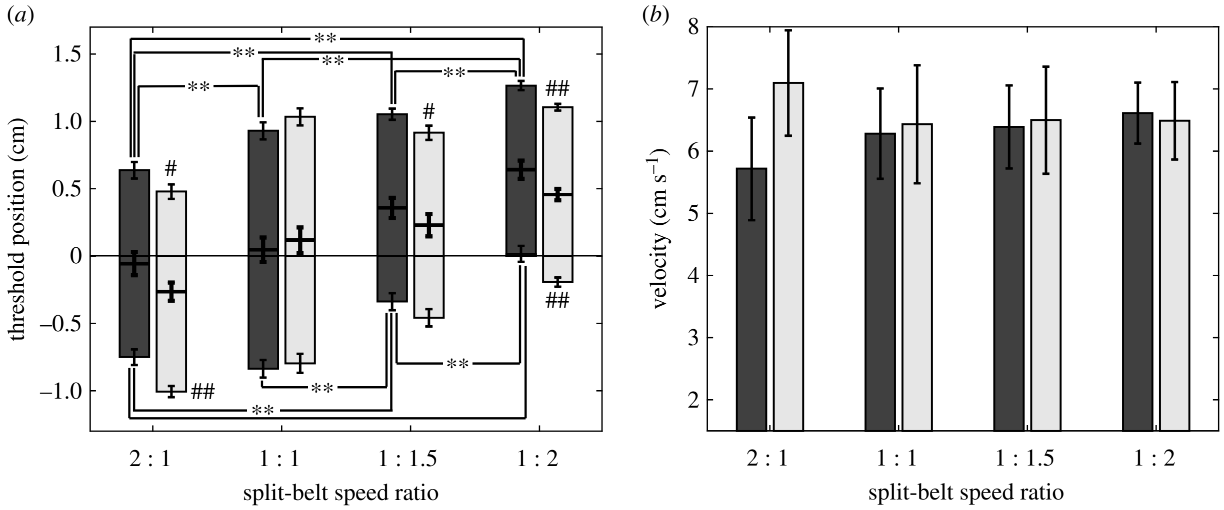

Figure 5. Estimated thresholds for initiation of ipsilateral double-support phases, s_L and s_R, and model velocity parameter q as function of belt speed ratio and anaesthesia. (*a*) Mean thresholds s_L (upper sides of bars) and s_R (lower sides of bars). The average (±s.e.) of the two thresholds is shown in the middle of each bar. (*b*) Model velocity parameter q. Means (±s.e.) were computed using Bayesian inference for each experimental condition. In each panel, a model parameter is shown for split-belt speed ratios 2 : 1, 1 : 1, 1 : 1.5 and 1 : 2. Dark grey bars show results for intact paws; light grey bars show results for anaesthetized right paws. Asterisks depict significant effects of the speed ratios (**$p < 0.01$); hashtags (#) depict significant effects of the unilateral anaesthesia ($^{\#}p < 0.05$, $^{\#\#}p < 0.01$).

example [36], as locomoting at lower speeds is less metabolically expensive [37].

The similarity of experimental and modelling results obtained in humans and cats walking on a split-belt treadmill suggests that there are common mechanisms of lateral balance control in these species. There are, however, some differences. In cats walking on a tied-belt and split-belt treadmill, there is a rather long phase of two-side support [1,22,38]; see also figures 1*a* and 2. By contrast, the human double-support phase is relatively short and justifiably neglected in inverted pendulum models of frontal plane walking dynamics [12,26]. The difference in the two-side support duration between cats and humans could potentially explain the lack of motor adaptation to asymmetric split-belt speeds in cats [33] as opposed to humans [39].

Using the inverted pendulum-based model, we also inferred the effect of anaesthesia application to right paws on model parameters, i.e. lateral stability thresholds. We found that both left and right stability thresholds undergo a symmetric shift towards the anaesthetized side regardless of the direction of belt speed difference (figures 6*b* and 7). As we explain next, these findings suggest that the central nervous system might use cutaneous feedback from paw pads to determine COM position with respect to the paws. Local anaesthetic injections in the foot sole effectively diminish cutaneous sensory feedback, resulting in the reduced sensation of pressure [40,41]. This might result in a false perception of unloading the paws on the anaesthetized side and thus a shift of body weight and COM position towards the contralateral side. Therefore, the animal may attempt to restore the body weight distribution between the left and right limbs by shifting the lateral stability thresholds on both sides of the body, such that perception of body weight distribution is even on the left and right paws. Thus, anaesthesia might alter sensory information used to estimate the position of the COM vertical projection within the borders of support. This inference suggests the potential importance of cutaneous feedback from paw pads in the balance control system, or, more specifically, the potential role of the nervous system in setting the lateral stability thresholds during locomotion.

It is possible to derive the relationship between the relative COM shift during unilateral paw anaesthesia and the shift in the perception threshold. Let us assume that a reduced cutaneous feedback from ipsilateral paws shifts a perceived COM location in the lateral direction. A COM compensatory shift to restore the pre-anaesthesia pressure distribution among the paws should be equal and opposite to the perceived COM shift. Thus, we can use the experimentally measured anaesthesia-evoked COM shift to define the extent of the cutaneous feedback reduction by anaesthesia of the ipsilateral paw pads. The relationship between the perceived COM shift and the cutaneous feedback reduction can be derived as described below.

If we neglect relatively small vertical accelerations of the body caused by limb extensions during walking in the cat, i.e. approximately $2\ \mathrm{m\ s^{-2}}$ (approx. 20% of acceleration of gravity; see fig. 3 in [42]), the sum of the vertical forces applied to the left and right paws from the ground is equal and opposite to mg:

$$F_L + F_R = mg, \tag{4.1}$$

where m is the cat's mass and g is the gravitational acceleration. Because the net rotation of the cat in the frontal plane during the whole walking cycle is zero, the net resultant moment of all forces acting on the cat in the frontal plane with respect to the COM must be zero in accordance with conservation of angular momentum. Then, assuming negligibly small ground reaction forces in the medial-lateral direction [5], the resultant moment with respect to the COM in the frontal plane is

$$0 = F_L(x + h) + F_R(x - h). \tag{4.2}$$

After solving for x, i.e. the COM position between the left (h) and right ($-h$) paws, we obtain

$$x = \frac{F_R - F_L}{F_L + F_R}\,h.$$

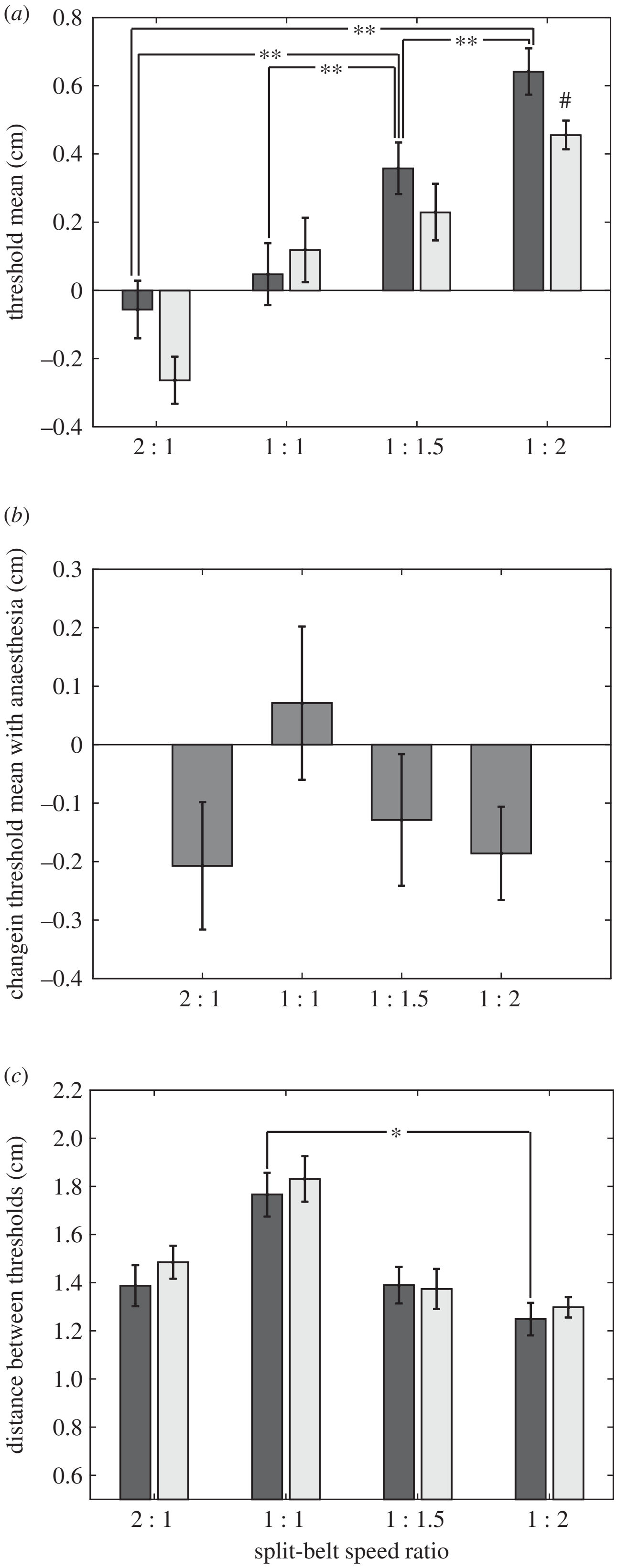

Figure 6. Estimated mean of thresholds s_L and s_R ($\pm$ s.e.), the change in threshold mean with anaesthesia, and the distance between thresholds as functions of belt speed ratio. (*a*) The threshold mean (the average of thresholds s_L and s_R). (*b*) The change in the threshold mean with the application of anaesthesia. (*c*) The distance between thresholds s_L and s_R. Means ($\pm$ s.e.) were computed using Bayesian inference for each experimental condition. In each panel, a model parameter is shown for split-belt speed ratios 2 : 1, 1 : 1, 1 : 1.5 and 1 : 2. Dark grey bars show results for intact paws; light grey bars show results for anaesthetized right paws. Asterisks depict significant effects of the speed ratio ($*p < 0.05$, $**p < 0.01$); hashtags (#) depict significant effects of the unilateral anaesthesia ($^{\#}p < 0.05$).

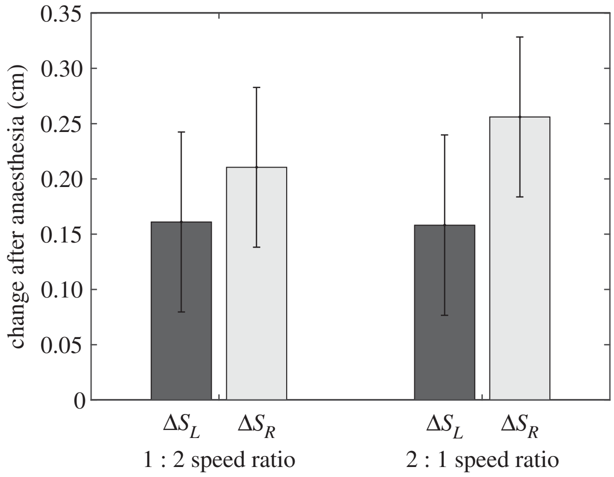

Figure 7. Effect of anaesthesia is independent of the sign of speed difference. The change in thresholds s_L and s_R owing to cutaneous anaesthesia applied to right paws for opposite split-belt speed ratios. Comparison shows no significant difference between the changes in thresholds s_L and s_R ($p > 0.05$) owing to anaesthesia for 1 : 2 and 2 : 1 speed ratios.

We define F'_R as the perceived load on ipsilateral paws after anaesthesia, where $F'_R < F_R$:

$$F'_R = F_R(1 - \delta). \tag{4.3}$$

Here, δ is a parameter that ranges from 0 to 1 and which represents the per cent reduction in load perception. The perceived COM position is defined as x':

$$x' = \frac{F'_R - F_L}{F_L + F'_R}\, h = \frac{F_R(1-\delta) - F_L}{F_L + F_R(1-\delta)}\, h. \tag{4.4}$$

Therefore, for small δ, the difference between the perceived and actual COM positions $\Delta x = x' - x$ can be approximately found as $\Delta x \approx -h\delta/2$. This bias in perception will lead to the apparent shift of the stability thresholds in the opposite direction: $\Delta s = -\Delta x \approx h\delta/2$. Thus, the contribution of cutaneous receptors to the load perception can be estimated as

$$\delta \approx \frac{2\Delta s}{h}. \tag{4.5}$$

Based on our inferences, the stability thresholds were shifted by anaesthesia by approximately 0.2 cm (figures 6*b* and 7) with the half distance between the paws of approximately 2.5 cm (figure 3), which suggests that cutaneous anaesthesia reduced the perception of the force by approximately 16%. This value appears rather small considering that paw pad anaesthesia completely eliminated withdrawal response to pinpricks in our experiments [1]. The relatively small reduction in perception of limb load after elimination of touch and pain sensation in paw pads suggests a substantial contribution to load perception from other load sensitive mechanoreceptors located throughout the limb including those responsible for osseoperception [43].

We found that the effect of anaesthesia may depend on the magnitude of speed ratio as the shift of the relative COM position and of lateral stability thresholds with anaesthesia perturbation was not significant in the 1 : 1 belt speed condition, but reached significance at higher belt speed ratios (figure 5*a*). The stronger effect of paw anaesthesia with increasing belt speed asymmetry is consistent with previous reports that bilateral removal of cutaneous feedback from cat hindpaws causes greater locomotor deficits in more demanding tasks (i.e. slope and horizontal ladder walking, walking with lateral perturbations) than in normal overground or tied-belt treadmill walking [29,44]. A possible interpretation of our results is that the balance control system's reliance on cutaneous feedback from the paws increases in unusual circumstances and more demanding tasks such as a large belt speed difference. Still, during normal cat walking, bilateral removal of hindpaw cutaneous feedback leads to modest changes in locomotor mechanics—lowering the pelvis, shortening step length and increasing the medial-lateral forces exerted by hindlimbs on the ground [29,44]. This indicates that cutaneous feedback from paws plays a role in lateral balance control. Removal of cutaneous feedback from feet in humans also affects lateral balance control [30,31]. Exact mechanisms by which cutaneous feedback from feet contribute to lateral balance control require additional studies. Cutaneous sensory input from various mechanoreceptors in the feet [45,46] is integrated at different levels of the nervous system from the spinal cord to somatosensory cortex [45]. Several studies of locomotion and standing in reduced animal preparations—decerebrate cats and rabbits—have demonstrated that mechanisms of automatic postural corrective responses to lateral body perturbations reside in the spinal cord, brainstem and cerebellum and that somatosensory feedback from the body limbs and trunk is sufficient for initiation and scaling the corrective responses [47,48].

In conclusion, this study demonstrated that lateral dynamics of cat COM during tied-belt and split-belt treadmill walking can be accurately described by augmenting the inverted pendulum model with the two-side support phase. We found that with increasing asymmetry in belt speeds, margins of dynamic stability on the faster and slower sides change asymmetrically. These results closely resemble the lateral COM dynamics during human walking, suggesting that the cat may be a suitable animal model to study neural mechanisms of lateral balance control during locomotion. In the present study, we obtained initial insights into a possible role of cutaneous feedback from paw pads. In particular, we demonstrated that unilateral removal of paw cutaneous feedback leads to a compensatory COM shift towards the anaesthetized side, but only in locomotor conditions with asymmetric belt speeds. In future studies, we plan to use similar experimental and modelling approaches to study effects of other sensory inputs on dynamic stability in the frontal and sagittal planes in walking cats.

Ethics. All experimental procedures were consistent with the Principles of Laboratory Animal Care (publication of the National Research Council of the National Academies, 8th edition, 2011) and approved by the Georgia Tech Institutional Animal Care and Use Committee.

Data accessibility. Original experimental data are available as the electronic supplementary material online at rs.figshare.com.

Authors' contributions. E.M.L. wrote the code to analyse experimental data; E.M.L. and W.H.B. processed data and conducted statistical analysis; H.P., A.N.K. and B.I.P. collected data; E.M.L., Y.I.M., H.P. and B.I.P. developed the study concept and experimental design; E.M.L., W.H.B. and Y.I.M. developed the model; E.M.L., W.H.B., B.I.P. and Y.I.M. wrote the original draft; all authors participated in writing the final draft.

Competing interests. We have no competing interests.

Funding. The Georgia Tech group was supported by NIH grant no. R01 HD32571 and DOD grant no. MR150051.

Acknowledgements. We would like to thank Dimitry Todorov and Robert Capps for their active participation in modelling and data analysis discussions.

References

1. Park H, Latash EM, Molkov YI, Klishko AN, Frigon A, DeWeerth SP, Prilutsky B. 2019 Cutaneous sensory feedback from paw pads affects lateral balance control during split-belt locomotion in the cat. *J. Exp. Biol.* **222**, 14. (doi:10.1242/jeb.198648)
2. Gray J. 1944 Studies in the mechanics of the tetrapod skeleton. *J. Exp. Biol.* **20**, 88–116.
3. Hof AL, Gazendam MG, Sinke WE. 2005 The condition for dynamic stability. *J. Biomech.* **38**, 1–8. (doi:10.1016/j.jbiomech.2004.03.025)
4. Fung J, Macpherson JM. 1995 Determinants of postural orientation in quadrupedal stance. *J. Neurosci.* **15**, 1121–1131. (doi:10.1523/JNEUROSCI.15-02-01121.1995)
5. Farrell BJ, Bulgakova MA, Sirota MG, Prilutsky BI, Beloozerova IN. 2015 Accurate stepping on a narrow path: mechanics, EMG, and motor cortex activity in the cat. *J. Neurophysiol.* **114**, 2682–2702. (doi:10.1152/jn.00510.2014)
6. Usherwood JR, Szymanek KL, Daley MA. 2008 Compass gait mechanics account for top walking speeds in ducks and humans. *J. Exp. Biol.* **211**, 3744–3749. (doi:10.1242/jeb.023416)
7. Willener AS, Handrich Y, Halsey LG, Strike S. 2016 Fat king penguins are less steady on their feet. *PLoS ONE* **11**, e0147784. (doi:10.1371/journal.pone.0147784)
8. Thompson NE, O'Neill MC, Holowka NB, Demes B. 2018 Step width and frontal plane trunk motion in bipedal chimpanzee and human walking. *J. Hum. Evol.* **125**, 27–37. (doi:10.1016/j.jhevol.2018.09.006)
9. MacKinnon CD, Winter DA. 1993 Control of whole body balance in the frontal plane during human walking. *J. Biomech.* **26**, 633–644. (doi:10.1016/0021-9290(93)90027-C)
10. O'Connor SM, Kuo AD. 2009 Direction-dependent control of balance during walking and standing. *J. Neurophysiol.* **102**, 1411–1419. (doi:10.1152/jn.00131.2009)
11. Townsend MA. 1985 Biped gait stabilization via foot placement. *J. Biomech.* **18**, 21–38. (doi:10.1016/0021-9290(85)90042-9)
12. Hof AL, van Bockel RM, Schoppen T, Postema K. 2007 Control of lateral balance in walking. Experimental findings in normal subjects and above-knee amputees. *Gait Posture* **25**, 250–258. (doi:10.1016/j.gaitpost.2006.04.013)
13. Pai YC, Patton J. 1997 Center of mass velocity-position predictions for balance control. *J. Biomech.* **30**, 347–354. (doi:10.1016/S0021-9290(96)00165-0)
14. Horak F, Macpherson J. 1996 *Postural orientation and equilibrium. Supplement 29. Handbook of physiology, exercise: regulation and integration of multiple systems*. New York, NY: Oxford.
15. Cavagna GA, Heglund NC, Taylor CR. 1977 Mechanical work in terrestrial locomotion: two basic mechanisms for minimizing energy expenditure. *Am. J. Physiol.* **233**, R243–R261. (doi:10.1152/ajpregu.1977.233.5.R243)
16. Griffin TM, Main RP, Farley CT. 2004 Biomechanics of quadrupedal walking: how do four-legged animals achieve inverted pendulum-like movements? *J. Exp. Biol.* **207**, 3545–3558. (doi:10.1242/jeb.01177)
17. Hildebrand M. 1968 Symmetrical gaits of dogs in relation to body build. *J. Morphol.* **124**, 353–360. (doi:10.1002/jmor.1051240308)
18. Dagg AI. 1974 The locomotion of the camel (*Camelus dromedarius*). *J. Zool.* **174**, 67–78. (doi:10.1111/j.1469-7998.1974.tb03144.x)
19. Basu C, Wilson AM, Hutchinson JR. 2019 The locomotor kinematics and ground reaction forces of walking

giraffes. *J. Exp. Biol.* **222**, jeb159277. (doi:10.1242/jeb.159277)

20. Pfau T, Hinton E, Whitehead C, Wiktorowicz-Conroy A RHJ. 2011 Temporal gait parameters in the alpaca and the evolution of pacing and trotting locomotion in the *Camelidae*. *J. Zool.* **283**, 193–202. (doi:10.1111/j.1469-7998.2010.00763.x)
21. Hildebrand M. 1980 The adaptive significance of tetrapod gait selection. *Am. Zool.* **20**, 255–267. (doi:10.1093/icb/20.1.255)
22. Wetzel MC, Atwater AE, Wait JV, Stuart DC. 1975 Neural implications of different profiles between treadmill and overground locomotion timings in cats. *J. Neurophysiol.* **38**, 492–501. (doi:10.1152/jn.1975.38.3.492)
23. Farrell BJ, Bulgakova MA, Beloozerova IN, Sirota MG, Prilutsky BI. 2014 Body stability and muscle and motor cortex activity during walking with wide stance. *J. Neurophysiol.* **112**, 504–524. (doi:10.1152/jn.00064.2014)
24. Blaszczyk J, Loeb GE. 1993 Why cats pace on the treadmill. *Physiol. Behav.* **53**, 501–507. (doi:10.1016/0031-9384(93)90144-5)
25. Roden-Reynolds DC, Walker MH, Wasserman CR, Dean JC. 2015 Hip proprioceptive feedback influences the control of mediolateral stability during human walking. *J. Neurophysiol.* **114**, 2220–2229. (doi:10.1152/jn.00551.2015)
26. Buurke TJW, Lamoth CJC, van der Woude LHV, Hof AL, den Otter R. 2019 Bilateral temporal control determines mediolateral margins of stability in symmetric and asymmetric human walking. *Sci. Rep.* **9**, 12494. (doi:10.1038/s41598-019-49033-z)
27. Buurke TJW, Lamoth CJC, Vervoort D, van der Woude LHV, den Otter R. 2018 Adaptive control of dynamic balance in human gait on a split-belt treadmill. *J. Exp. Biol.* **221**, jeb174896.
28. Ting LH, Macpherson JM. 2004 Ratio of shear to load ground-reaction force may underlie the directional tuning of the automatic postural response to rotation and translation. *J. Neurophysiol.* **92**, 808–823. (doi:10.1152/jn.00773.2003)
29. Bolton DA, Misiaszek JE. 2009 Contribution of hindpaw cutaneous inputs to the control of lateral stability during walking in the cat. *J. Neurophysiol.* **102**, 1711–1724. (doi:10.1152/jn.00445.2009)
30. Perry SD, McIlroy WE, Maki BE. 2000 The role of plantar cutaneous mechanoreceptors in the control of compensatory stepping reactions evoked by unpredictable, multi-directional perturbation. *Brain Res.* **877**, 401–406. (doi:10.1016/S0006-8993(00)02712-8)
31. Meyer PF, Oddsson LI, De Luca CJ. 2004 Reduced plantar sensitivity alters postural responses to lateral perturbations of balance. *Exp. Brain Res.* **157**, 526–536. (doi:10.1007/s00221-004-1868-3)
32. Prilutsky BI, Sirota MG, Gregor RJ, Beloozerova IN. 2005 Quantification of motor cortex activity and full-body biomechanics during unconstrained locomotion. *J. Neurophysiol.* **94**, 2959–2969. (doi:10.1152/jn.00704.2004)
33. Kuczynski V *et al.* 2017 Lack of adaptation during prolonged split-belt locomotion in the intact and spinal cat. *J. Physiol.* **595**, 5987–6006. (doi:10.1113/JP274518)
34. Onushko T, Boerger T, Van Dehy J, Schmit BD. 2019 Dynamic stability and stepping strategies of young healthy adults walking on an oscillating treadmill. *PLoS ONE* **14**, e0212207. (doi:10.1371/journal.pone.0212207)
35. Young PM M, Dingwell JB. 2012 Voluntary changes in step width and step length during human walking affect dynamic margins of stability. *Gait Posture* **36**, 219–224. (doi:10.1016/j.gaitpost.2012.02.020)
36. Finley JM, Bastian AJ, Gottschall JS. 2013 Learning to be economical: the energy cost of walking tracks motor adaptation. *J. Physiol.* **591**, 1081–1095. (doi:10.1113/jphysiol.2012.245506)
37. Taylor CR, Heglund NC, Maloiy GM. 1982 Energetics and mechanics of terrestrial locomotion. I. Metabolic energy consumption as a function of speed and body size in birds and mammals. *J. Exp. Biol.* **97**, 1–21. (doi:10.1146/annurev.ph.44.030182.000525)
38. Frigon A, Thibaudier Y, Hurteau MF. 2015 Modulation of forelimb and hindlimb muscle activity during quadrupedal tied-belt and split-belt locomotion in intact cats. *Neuroscience* **290**, 266–278. (doi:10.1016/j.neuroscience.2014.12.084)
39. Torres-Oviedo G, Vasudevan E, Malone L, Bastian AJ. 2011 Locomotor adaptation. *Prog. Brain Res.* **191**, 65–74. (doi:10.1016/B978-0-444-53752-2.00013-8)
40. Mackenzie RA, Burke D, Skuse NF, Lethlean AK. 1975 Fibre function and perception during cutaneous nerve block. *J. Neurol. Neurosurg. Psychiatry* **38**, 865–873. (doi:10.1136/jnnp.38.9.865)
41. Hogan QH, Abram SE. 1997 Neural blockade for diagnosis and prognosis. A review. *Anesthesiology* **86**, 216–241. (doi:10.1097/00000542-199701000-00026)
42. Manter JT. 1938 The dynamics of quadrupedal walking. *J. Exp. Biol.* **15**, 522–540.
43. Macefield VG. 2005 Physiological characteristics of low-threshold mechanoreceptors in joints, muscle and skin in human subjects. *Clin. Exp. Pharmacol. Physiol.* **32**, 135–144. (doi:10.1111/j.1440-1681.2005.04143.x)
44. Bouyer LJ, Rossignol S. 2003 Contribution of cutaneous inputs from the hindpaw to the control of locomotion. I. Intact cats. *J. Neurophysiol.* **90**, 3625–3639. (doi:10.1152/jn.00496.2003)
45. Abraira VE, Ginty DD. 2013 The sensory neurons of touch. *Neuron* **79**, 618–639. (doi:10.1016/j.neuron.2013.07.051)
46. Strzalkowski NDJ, Peters RM, Inglis JT, Bent LR. 2018 Cutaneous afferent innervation of the human foot sole: what can we learn from single-unit recordings? *J. Neurophysiol.* **120**, 1233–1246. (doi:10.1152/jn.00848.2017)
47. Musienko PE, Zelenin PV, Lyalka VF, Orlovsky GN, Deliagina TG. 2008 Postural performance in decerebrated rabbit. *Behav. Brain Res.* **190**, 124–134. (doi:10.1016/j.bbr.2008.02.011)
48. Musienko P, Courtine G, Tibbs JE, Kilimnik V, Savochin A, Garfinkel A, Roy RR, Edgerton VR, Gerasimenko Y. 2012 Somatosensory control of balance during locomotion in decerebrated cat. *J. Neurophysiol.* **107**, 2072–2082. (doi:10.1152/jn.00730.2011)